

A Comparison between Coupled SPH-DEM and LBM-DEM Approaches for Soil Liquefaction

**Saman Farzi Sizkow,¹ and
Usama El Shamy, Ph.D., P.E., M.ASCE¹**

¹ Department of Civil and Environmental Engineering, Southern Methodist University, Dallas, TX 75205; e-mail: sfarzisizkow@mail.smu.edu, uelshamy@lyle.smu.edu

ABSTRACT

In this paper, the liquefaction of saturated granular soil subjected to dynamic base excitation is evaluated using fully particle-based SPH-DEM approach and the obtained results are compared to the results of pore-scale LBM-DEM technique. It is observed that the deposit liquefied during the application of strong base excitations as a result of reduction in porosity that led to pore pressure buildup and subsequent decrease of average particle coordination number and degradation of soil strength and stiffness. The comparison performed between the two methods also shows that the results of the computationally cheaper SPH-DEM approach are fairly consistent with the outcomes of highly accurate LBM-DEM technique.

INTRODUCTION

Numerous attempts have been made at incorporating fluid-particle interaction equations into discrete element method formulation. Two popular coupling techniques are: (1) to describe the fluid flow by averaged Navier-Stokes equation based on mean multiphase mixture properties and employ well-established semi-empirical equations to calculate the fluid particle interaction forces (El Shamy and Zeghal, 2005, El Shamy et al., 2010, Ravichandran et al., 2010) and (2) to model fluid at the pore-scale level to investigate the development of pore pressure due to actual changes in the shape and volume of the pore space caused by particle movements. The pore-scale methods benefit from high accuracy that comes at the price of being computationally expensive. One of the popular pore-scale approaches is achieved by coupling lattice Boltzmann and discrete element methods (LBM-DEM) which is used by various researchers to study different phenomena (Han and Cundall, 2011, El Shamy and Abdelhamid, 2014, Abdelhamid and El Shamy, 2016).

In recent years a new coupled smoothed particle hydrodynamics and discrete element method (SPH-DEM) scheme has been developed that, instead of modeling the fluid flow at the pore scale, uses averaged Navier-Stokes equations to describe the fluid phase behavior and well-established semi-empirical formulas for fluid-particle interactions (Sun et al., 2013, Robinson et al., 2014, He et al., 2018, Markauskas et al., 2018). This method has the advantage of being

computationally far less demanding compared to pore-scale models and due to its meshless nature is very well-suited for large strain and deformable boundary problems.

This paper aims to conduct a comparison between SPH-DEM and LBM-DEM approaches to evaluate the accuracy of the relatively new SPH-DEM technique which requires much less computational resources compared to high-accuracy pore-scale LBM-DEM method. To this end, a saturated granular deposit with microscale and macroscale properties similar to the one employed by El Shamy and Abdelhamid (2014) was created using the proposed SPH-DEM approach. The dynamic response of the deposit to high amplitude base excitations was analyzed and compared to the results presented by El Shamy and Abdelhamid (2014). The obtained results suggest that the liquefaction is a result of reduction in void spaces during strong ground motions leading to high pore pressure buildup and consequent loss of interparticle contacts and degradation of soil strength and stiffness. It is also observed that the two approaches yield relatively similar results. In addition, the SPH-DEM simulation took approximately 2 hours to finish while the original simulation conducted using the user-written, serial LBM-DEM code running on the same computer, needed around two weeks. Obviously, parallelizing the LBM-DEM code can significantly improve its performance, however, the gap between the computational costs of the two techniques still remains huge.

COUPLED SPH-DEM APPROACH

In SPH scheme, the fluid domain is discretized into a set of individual particles carrying local properties of the fluid such as density and pressure. The fluid pressure is obtained from the weakly compressible equation of state. The phase coupling is achieved through semi-empirical relationships between the fluid-particle interaction forces and parameters such as the local porosity and relative velocity between the two phases. An explicit time integration scheme is used to solve the equation of motion for both solid and fluid particles. Details of the model could be found in El Shamy and Siskow (2020).

COUPLED LBM-DEM APPROACH

For the solid particles and fluid mixture, the fluid equations as well as the momentum equations for each particle are solved using an explicit time integration scheme. The fluid is idealized at pore-scale using lattice Boltzmann method, and fluid variables such as velocity and pressure are obtained at fixed grid points. A nonslip fluid boundary condition is applied at the particle surface to maintain compatibility between the fluid phase and solid phase. The fluid hydromechanical forces are calculated based on the momentum exchange between the fluid and the particles (El Shamy and Abdelhamid, 2014).

MODEL PROPERTIES

The simulation was conducted on a 190 mm high (in model units) saturated deposit. The lateral dimensions of the periodic deposits were chosen to be 48×48 mm. The particle size range of 4.8 mm to 7.2 mm, was used in the creation of the deposits. High gravitational field of 30g was employed to decrease the dimensions of the domain. The saturated unit weight of the deposits was

determined to be around 19.3 kg/m^3 . To saturate the deposits, a fluid column with a height of 200 mm and lateral dimensions of $48 \times 48 \text{ mm}$ was built within the periodic domain using SPH particles. The high fluid viscosity of 0.166 Pa.s was used here to account for the large particle sizes and to achieve a permeability close to that of coarse sand. The shear wave velocity and low strain shear modulus of the final deposit were determined to be approximately 179 m/s and 65 MPa which are close to those of the benchmark deposit (El Shamy and Abdelhamid, 2014). A 3D view of the saturated deposit is shown in Figure. 1.

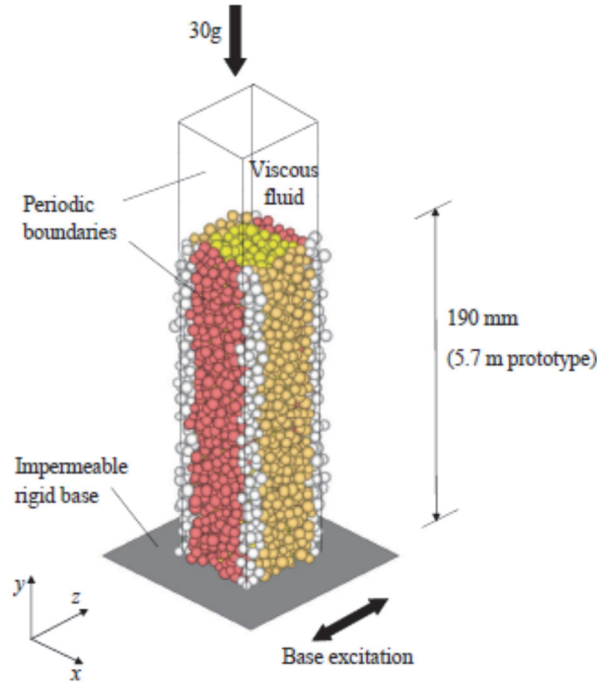


Figure 1. 3D view of saturated granular deposit.

RESULTS

The deposit was subjected to a sinusoidal base excitation with amplitude of $0.25g$ and frequency of 3 Hz . The sinusoidal input signal gradually increases until it reaches the maximum acceleration amplitude at 4.5 s , where it remains constant for an additional 7.5 s before it gradually decreases to zero at 13 s . Different parameters were recorded during the application of the seismic loading at various depth locations. The time histories of excess pore pressure ratio (the ratio of the excess pore pressure to the initial vertical effective stress) at different depth locations inside the deposit are shown in Figure 2. The results show consistency between the two approaches. It can be seen that the pore pressure buildup first occurred in the shallow layers of the deposit and then propagated downward. According to this figure, the excess pore pressure ratio of 1.0 was reached at the point located approximately 1 m below the surface. The excess pore pressure ratio in the top layer was smaller than 1.0 . This can be attributed to the fact that this layer is located very close to the free fluid surface that leads to quick dissipation of the excess pore pressure.

Figure 3 shows the time histories of porosities at different depth locations. The recorded data shows a general decrease in the porosity in all layers during the simulations. The average particle acceleration at different depths along the vertical axis of the deposit was recorded and is presented in Figure 4. It was observed that the acceleration of the top 2.5 m of the deposit noticeably diminished after the onset of the liquefaction. This drop in the acceleration amplitude is more evident in the top 1 m of the deposit. Comparing the two sets of results also shows similar acceleration patterns.

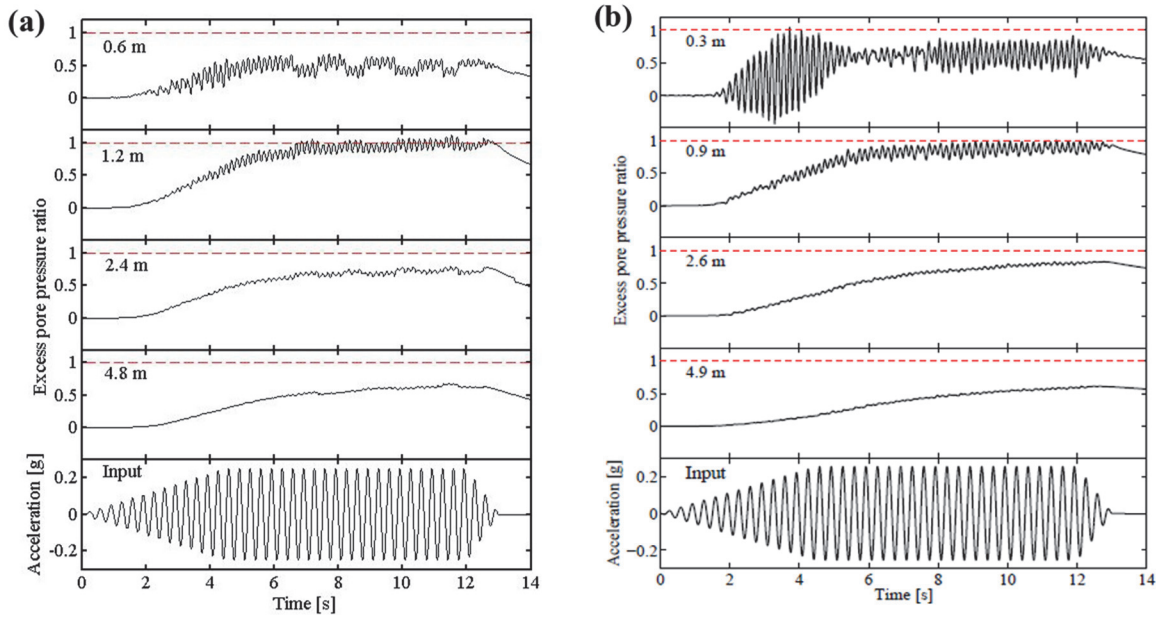


Figure 2. Time histories of excess pore water pressure at the selected depths obtained from (a) SPH-DEM and (b) LBM-DEM.

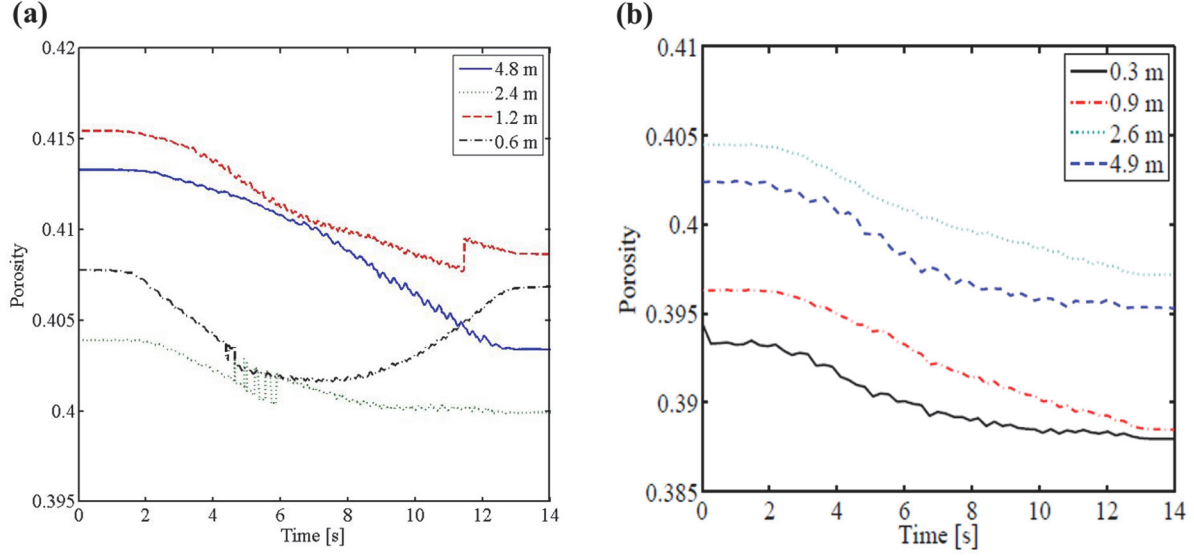


Figure 3. Time histories of porosities at the selected depths obtained from (a) SPH-DEM and (b) LBM-DEM.

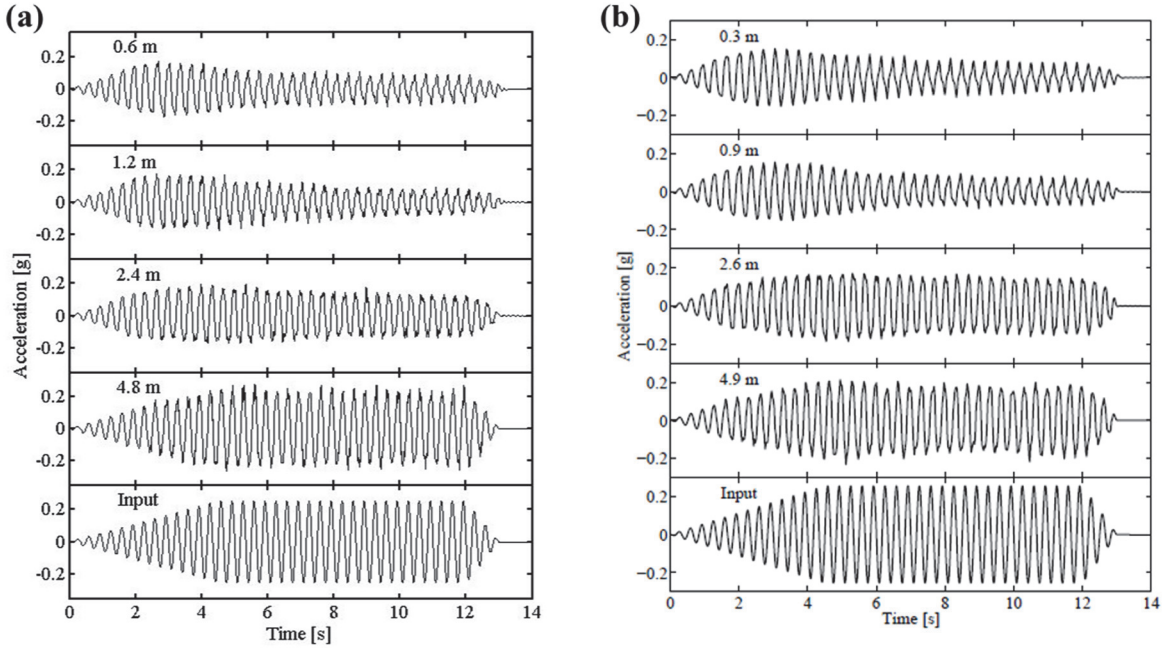


Figure 4. Time histories of average horizontal acceleration at the selected depths obtained from (a) SPH-DEM and (b) LBM-DEM.

To explain the observed acceleration patterns at a microscale level, time histories of the averaged coordination number and the drag forces normalized by the average weight of particles are provided in Figure 5 and Figure 6, respectively. Figure 6 shows that the normalized drag force

drastically increased during the shaking and reached the value of 1.0 for the upper strata. It can be seen from Figure 5 that as the drag forces on the particles increased, the number of contacts between them significantly dropped, especially for the top layers where the coordination number reached values lower than 4 which is the threshold value for the stability of a sphere packing. For the bottom layer the fluid drag force was not large enough to create significant separation between the particles and, as it is evident from Figure 5, the coordination number did not drop significantly below 4 and as a result, the decrease in the average particle acceleration was quite small at this depth.

The cyclic shear stress-shear strain loops are presented in Figure 7. A progressive degradation of the soil stiffness and a gradual decrease in the shear modulus can be seen. In addition, Figure 7 shows that the two approaches deliver fairly similar results in terms of maximum amplitudes of the cyclic shear strain and cyclic shear stress as well as the severity of stiffness degradation at different depths. Figure 8 shows the plots of the cyclic shear stress versus the effective confining stress. It is evident that both techniques predict that the effective confining stress completely vanishes in the top 1 m of the deposit by the end of loading.

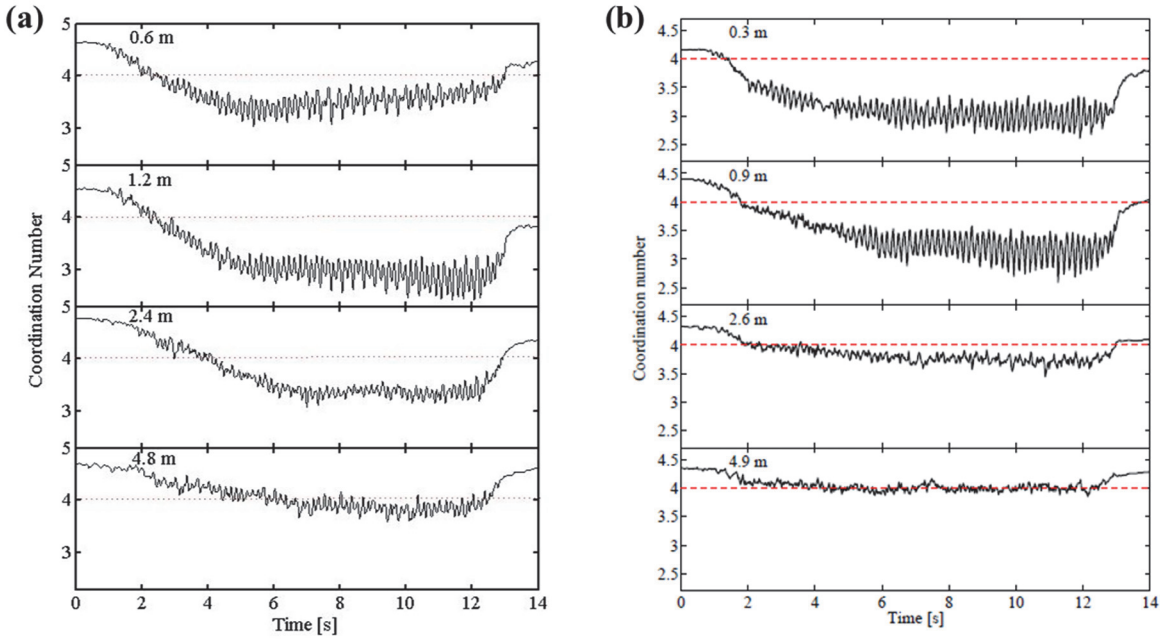


Figure 5. Time histories of coordination number at the selected depths obtained from (a) SPH-DEM and (b) LBM-DEM.

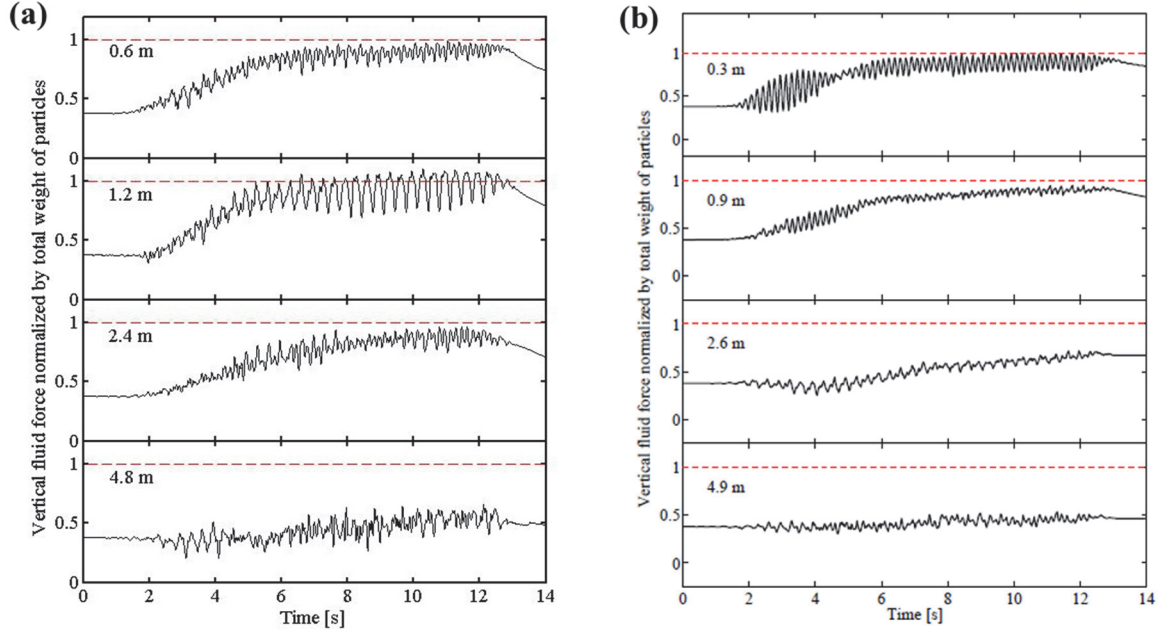


Figure 6. Time histories of normalized drag force at the selected depths obtained from (a) SPH-DEM and (b) LBM-DEM.

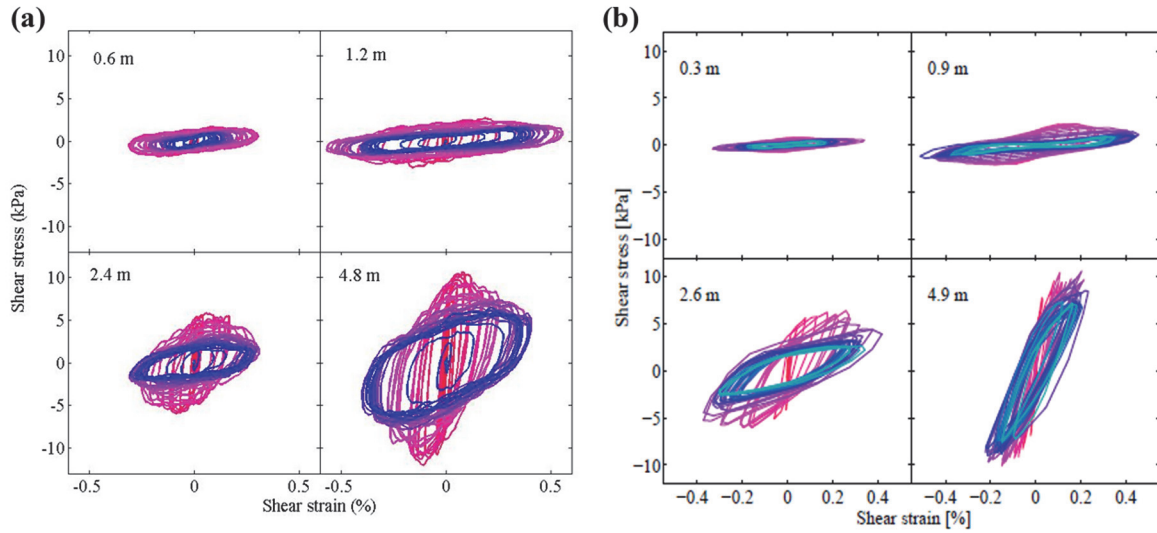


Figure 7. Shear stress-shear strain loops at selected depth location obtained from (a) SPH-DEM and (b) LBM-DEM.

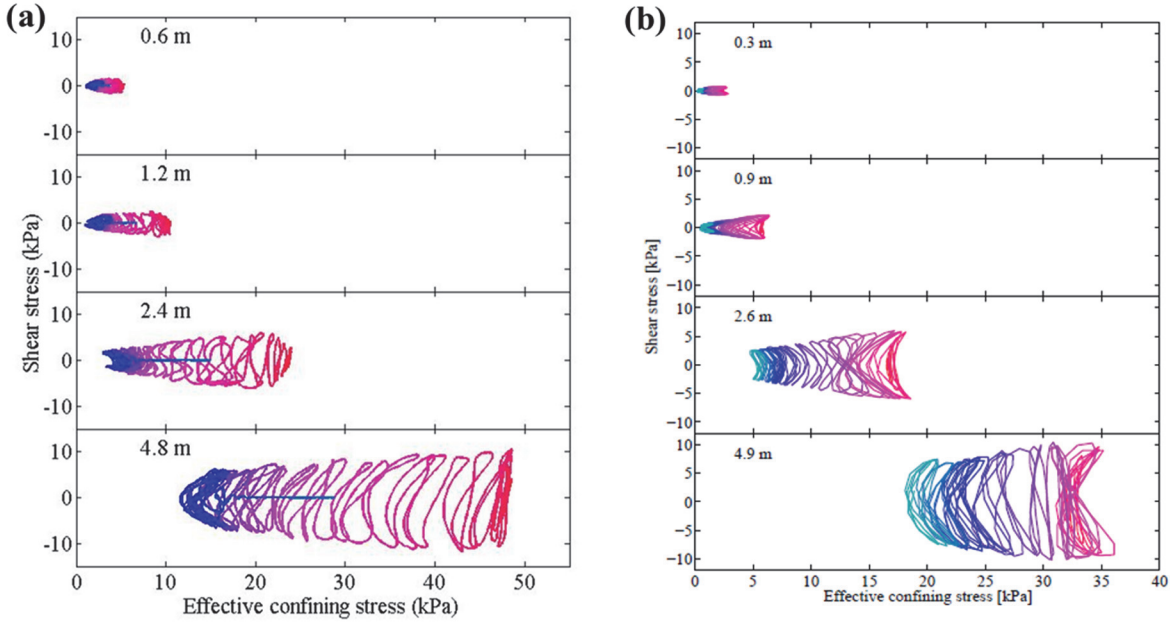


Figure 8. Effective stress path at selected depth location obtained from (a) SPH-DEM and (b) LBM-DEM.

CONCLUSION

The proposed SPH-DEM approach was used to model the response of saturated soil deposits subjected to seismic excitation. The results show that the liquefaction took place in the deposit marked by several response mechanisms including excess pore-pressure buildup approaching the value of one, increase in the vertical drag forces that counterbalance the weight of solid particles, reduction of averaged coordination number causing the instability of the packing, diminishing averaged particle acceleration time histories and continuous degradation of soil stiffness and strength. Furthermore, the comparison conducted between the results of the presented technique and those of high-accuracy pore-scale LBM-DEM approach reveals fairly consistent patterns.

ACKNOWLEDGMENT

This research was partially supported by the National Science Foundation awards number CMMI-1728612 and CMMI-1000908. This support is gratefully acknowledged.

REFERENCES

Abdelhamid, Y. and El Shamy, U. (2016). "Pore-scale modeling of fine-particle migration in granular filters." *International Journal of Geomechanics*, 16(3), 04015086.

- El Shamy, U. and Abdelhamid, Y. (2014). "Modeling granular soils liquefaction using coupled lattice Boltzmann method and discrete element method." *Soil Dynamics and Earthquake Engineering*, 67, 119-132.
- El Shamy, U. and Zeghal, M. (2005). "Coupled continuum-discrete model for saturated granular soils." *Journal of engineering mechanics*, 131(4), 413-426.
- El Shamy, U., Zeghal, M., Dobry, R., Thevanayagam, S., Elgamal, A., Abdoun, T., Medina, C., Bethapudi, R. and Bennett, V. (2010). "Micromechanical aspects of liquefaction-induced lateral spreading." *International Journal of Geomechanics*, 10(5), 190-201.
- El Shamy, U., and Sizkow, S.F. (2020). "Coupled smoothed particle hydrodynamics-discrete element method simulations of soil liquefaction and its mitigation using gravel drains." *Soil Dynamics and Earthquake Engineering* (Accepted).
- Han, Y. and Cundall, P.A. (2011). "Lattice Boltzmann modeling of pore-scale fluid flow through idealized porous media." *International Journal for Numerical Methods in Fluids*, 67(11), 1720-1734.
- He, Y., Bayly, A.E., Hassanpour, A., Muller, F., Wu, K. and Yang, D. (2018). "A GPU-based coupled SPH-DEM method for particle-fluid flow with free surfaces." *Powder technology*, 338, 548-562.
- Markauskas, D., Kruggel-Emden, H. and Scherer, V. (2018). "Numerical analysis of wet plastic particle separation using a coupled DEM-SPH method." *Powder Technology*, 325, 218-227.
- Ravichandran, N., Machmer, B., Krishnapillai, H. and Meguro, K. (2010). "Micro-scale modeling of saturated sandy soil behavior subjected to cyclic loading." *Soil Dynamics and Earthquake Engineering*, 30(11), 1212-1225.
- Robinson, M., Ramaioli, M. and Luding, S. (2014). "Fluid-particle flow simulations using two-way-coupled mesoscale SPH-DEM and validation." *International journal of multiphase flow*, 59, 121-134.
- Sun, X., Sakai, M. and Yamada, Y. (2013). "Three-dimensional simulation of a solid-liquid flow by the DEM-SPH method." *Journal of Computational Physics*, 248, 147-176.